PKR-mediated Stress Response Enhances Dengue and Zika Virus Replication

Taissa Ricciardi-Jorge[1*], Edroaldo Lummertz da Rocha[1], Edgar Gonzalez-Kozlova[1,2], Gabriela Flavia Rodrigues-Luiz[1], Brian J Ferguson[2], Nerea Irigoyen[2], Daniel Santos Mansur[1*]

[1] Departamento de Microbiologia, Imunologia e Parasitologia, Centro de Ciências Biológicas (CCB), Universidade Federal de Santa Catarina (UFSC), Florianópolis, SC, Brasil.

[2] Present address, Icahn School of Medicine, New York, USA.

[3] Department of Pathology, University of Cambridge, Tennis Court Road, Cambridge, UK.

* Corresponding authors: daniel.mansur@ufsc.br; t.ricciardi.jorge@gmail.com

ABSTRACT

The mechanisms by which *Flaviviruses* use non-canonical translation to support their replication in host cells are largely unknown. Here we investigated how the integrated stress response (ISR), which promotes translational arrest by eIF2α phosphorylation (p–eIF2α), regulates *Flavivirus* replication. During Dengue virus (DENV) and Zika virus (ZIKV) infection, eIF2α activation peaked at 24 hours post infection and was dependent on PKR but not type I interferon. The ISR is activated downstream of p-eIF2α during infection with either virus, but translation arrest only occurred following DENV infection. Despite this difference, both DENV and ZIKV replication was impaired in cells lacking PKR, independent of IFN-I/NF-kB signaling or cell viability. By using a ZIKV 5'UTR reporter system as a model, we found that this region of the genome is sufficient to promote an enhancement of viral mRNA translation in the presence of an active ISR. Together we provide evidence that *Flaviviruses* escape ISR translational arrest and co-opt this response to increase viral replication.

INTRODUCTION

The Flavivirus genus is part of the *Flaviviridae* family and contains the causative agents of several human diseases of high global impact, such as: DENV, ZIKV, Japanese encephalitis virus (JEV), yellow fever virus (YFV), West Nile virus (WNV) and others. Flaviviruses are enveloped ssRNA(+)viruses of about 50 nm in diameter with 10-11 kb genome containing a single ORF flanked by two non-coding segments (UTRs) 5´- (capped) and 3'- (non-polyadenylated) [1]. Flavivirus replication is cytoplasmic in strong association with ER, forming viral replication complexes by convolution of ER membrane [2].

Despite the presence of a 5´-cap on its genome, DENV has been shown to use a cap-independent mechanism for protein synthesis under the suppression of cap-binding protein, eIF4E [3]. Using DENV and ZIKV, this mechanism was later shown to be mediated by an internal ribosomal entry site (IRES localized in viral -UTR [4]. A recent report has confirmed the existence of the IRES element [5], indicating, along with previous suggestions [3,6,7] that a cap-dependent translation would be used for viral polyprotein synthesis until the suppression of canonical translation initiation when a switch to cap-independent translation would take place. This alternative cap-independent mechanism, including cell conditions to promote the switch in translation mode, remains to be fully characterized.

A well-known cellular control over the translation machinery is coordinated by four kinases of the integrated stress response (ISR), that act as sensors of different stressors. They are: (i) PKR, activated by dsRNA; (ii) HRI, activated by oxidative stress and/or heme deficiency; (iii) PERK, activated by reticulum stress; and (iv) GCN2, activated by deprivation of amino acids [8–10]. Therefore, ISR is capable of detecting viral infections directly by ligating replication intermediates (dsRNA) or indirectly via structural or metabolic stresses. A shared target of these four kinases is the subunit alpha of the translation factor eIF2 (eIF2α), which is part of the ternary complex (TC, eIF2-GTP-$tRNA_i^{Met}$), necessary for translation initiation. Phosphorylation of eIF2α (p-eIF2α) prevents the exchange of the associated inactive GDT for the active GTP, blocking its recycling for participation in the formation of new 43S complexes, thus inhibiting general cell translation [11,12].

In the present work, we show that PKR is the main kinase leading to eIF2α phosphorylation and cellular protein translation arrest during DENV/ZIKV infection. This event, however, is linked to the establishment of an optimal cellular environment for virus replication. Using ZIKV as a model, we demonstrate that eIF2α phosphorylation requires viral 5´-UTR to promote enhanced viral translation. These results suggest that ISR may provide the conditions necessary for viral alternative translation boosting viral replication.

68 **RESULTS**

69 **DENV4 and ZIKV can induce ISR activation during infection**

70 Interferon stimulated genes are central for Flavivirus restriction, therefore we used human
71 lung A549 cells, as they support DENV and ZIKV replication and also produce and respond to type one
72 interferons (IFN-I) [4,13–17]. We evaluated eIF2α phosphorylation during DENV4 and ZIKV
73 infection as a marker of ISR activation by these viruses. By immunoblot analysis, we show that both
74 viruses induce p–eIF2α by 24 hours post infection (h p.i.) (Figure 1A). This time point coincides with
75 PKR activation by autophosphorylation (Thr451), which suggests the participation of this kinase in ISR
76 activation. Quantification by flow cytometry enables us to determine that eIF2α phosphorylation
77 happens after 12 h p.i. reaching a peak at 24 h p.i. (Figure 1B). This time frame is surprisingly late,
78 considering that from at least 12 h p.i. infectious virus particles can already be detected in cell
79 supernatants under these experimental conditions (Supplementary Figure 1).

80 To further investigate the context of eIF2α phosphorylation, cells were co-stained with a
81 monoclonal antibody directed against the flavivirus envelope protein (Figure 1C-D). At 24 h p.i.
82 DENV4 infected cells exhibited a significant double-positive population, with about 90% of p–eIF2α+
83 cells being infected. However, during ZIKV infection, there is a lower proportion of double-positive
84 cells, with about 40% of envelope positive cells in the p–eIF2α+ population. These cells may be infected
85 with ZIKV, but they do not yet express enough envelope protein to allow detectable staining. The same
86 profile of co-staining quantified by cytometry could also be visualized by immunofluorescence (Figure
87 1D).

88 In summary, although both infections led to different profiles of anti–p–eIF2α and anti–
89 flavivirus co-staining, both viruses promote stress responses within the same time frame.

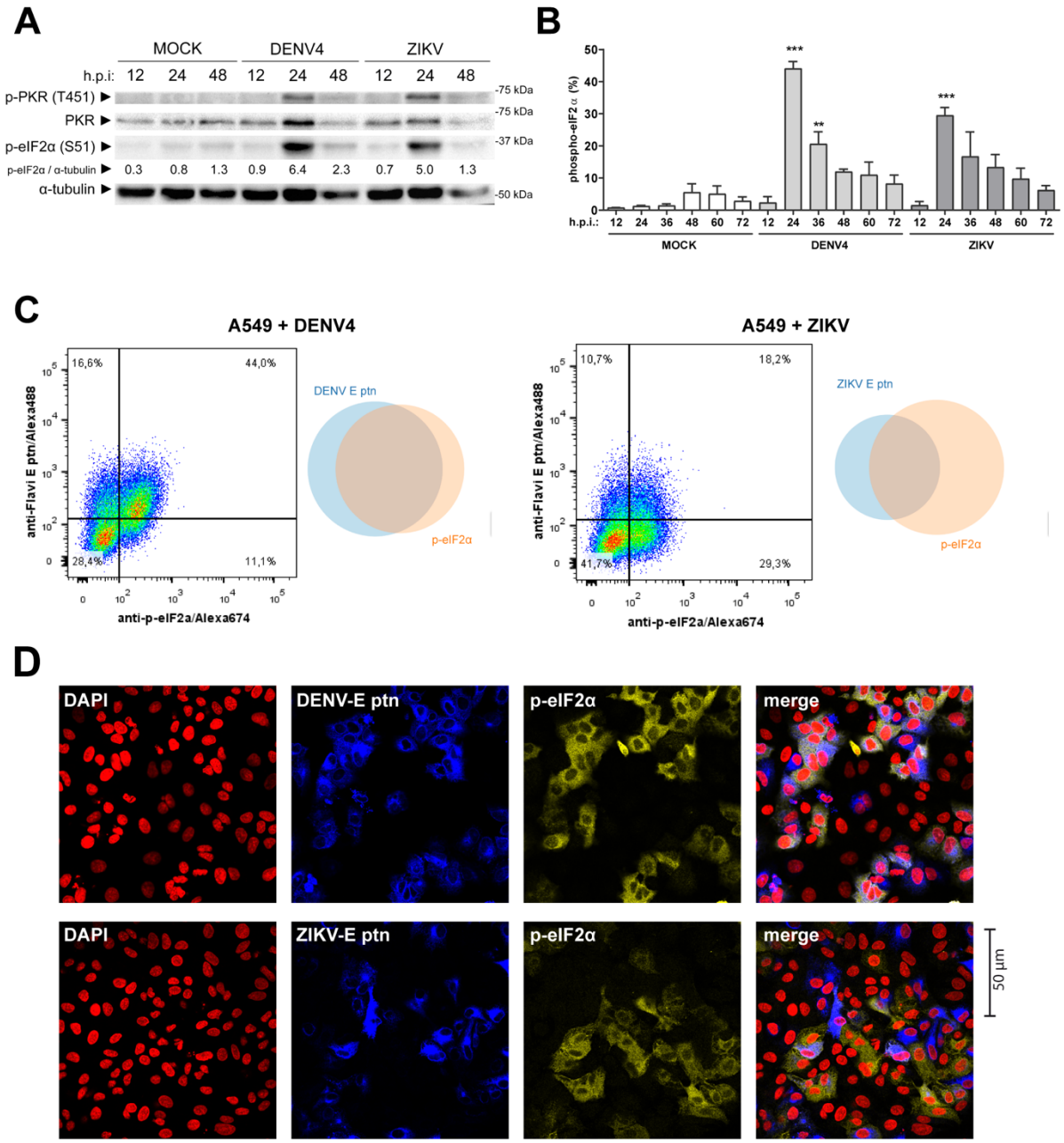

Figure 1 – DENV4 and ZIKV promote phosphorylation of eIF2α in A549 cells. A549 cells were infected with DENV4 (MOI 2) or ZIKV (MOI 3) and harvested at the indicated times for analysis. (A) Immunoblot analysis of cell extracts resolved in denaturing SDS-PAGE. (B) Flow cytometry analysis for quantification of cells expressing p–eIF2α within the total population (C) Dot plot and Venn diagram of representative results from co-staining with anti-Flavivirus E protein and anti-p–eIF2α at 24 h p.i. analysed by flow cytometry and (D) immunofluorescence of infections under the same conditions, representative images of three independent experiments. In the column chart, the bars represent the means ± SEM from three independent experiments. Statistical analysis was performed by paired *t* test comparing infected samples to the respective uninfected control. *: $p \leq 0.05$; **: $p \leq 0.01$; ***: $p \leq 0.001$; ns / no markup: no statistical difference; h p.i: hours post-infection.

Phosphorylation of eIF2α during DENV4/ZIKV infection is PKR-dependent and IFN-I independent

To investigate which ISR kinase promotes eIF2α phosphorylation in our model, gene deletion by CRISPR-Cas9 was used to produce A549 PKR and IFNAR knockout cell lines. In PKR$^{-/-}$ cells (Supplementary Figure 2A) infected with DENV4 or ZIKV p–eIF2α was abrogated indicating that ISR activation promoted by both viruses is mostly dependent on this kinase (Figure 2A,B). Since PKR is an IFN-stimulated gene (ISG), and considering the late ISR activation, the participation of IFN-I signalling in eIF2α phosphorylation was assessed. However, there was no change in the level of p–eIF2α in infected IFNAR$^{-/-}$ A549s compared to WT cells (Figure 2A,B). Likewise, experiments using a PKR/IFNAR double-knockout (Supplementary Figure 2B) lineage confirmed the requirement for constitutive PKR expression to drive eIF2α phosphorylation.

The persistence of a small population p–eIF2α+ in the PKR$^{-/-}$ cells infected with ZIKV, indicates the activation of other ISR kinase by this virus. To investigate PERK activity, a selective inhibitor, GSK2656157 [18], was used. GSK2656157 treatment did not alter the induction of p–eIF2α in DENV4 infected cells but promoted a small decrease in p–eIF2α population in ZIKV infected cells (Figure 2C). This demonstrates a minor participation of PERK in the ISR activation in the ZIKV model.

In summary, the phosphorylation of eIF2α during infection by DENV4 or ZIKV is mainly PKR dependent and IFN-I independent in this model.

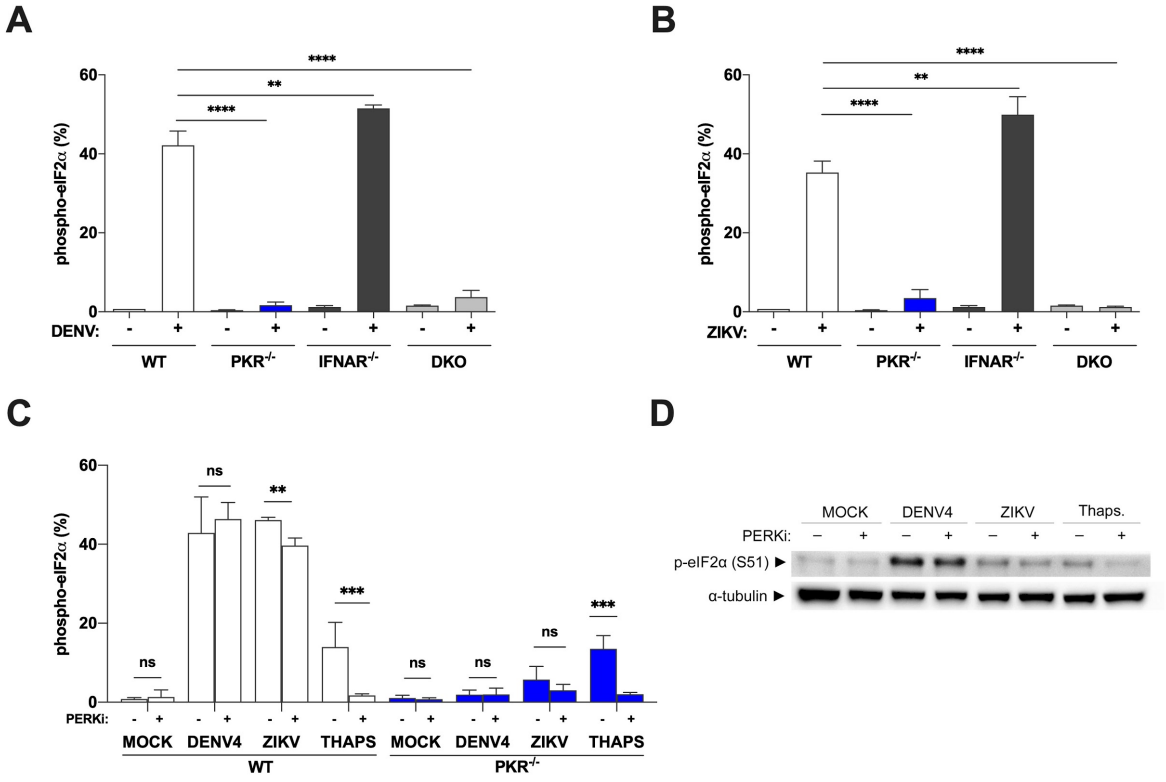

120 **Figure 2 – Phosphorylation of eIF2α during DENV4 or ZIKV infections is PKR-dependent and**
121 **IFN-independent**. (A) Flow cytometry analysis for quantification of cells expressing p–eIF2α within
122 the total population of the indicated lineages of A549 cells infected with DENV4 (MOI 2) at 24 h p.i.;
123 and (B) same experiment using ZIKV (MOI 3) (C) Flow cytometry analysis for quantification of cells
124 expressing p–eIF2α within the total population A549 WT and $PKR^{-/-}$cells infected with DENV4 (MOI
125 2) or ZIKV (MOI 3) or treated with thapsigargin 2μM for 45 minutes in the presence or absence of the
126 PERK inhibitor GSK2656157 (5 μM) for 24h; and (D) immunoblot analysis of cell extracts from the
127 same experiment resolved in denaturing SDS-PAGE. Representative image of two independent
128 experiments. DKO: double $IFNAR^{-/-}/PKR^{-/-}$ knockout. In column charts, bars represent the mean ± SEM
129 from three independent experiments. Statistical analysis was performed by one-way ANOVA, followed
130 by Tukey's test for multiple comparisons.*: $p \leq 0.05$; **: $p \leq 0.01$; ***: $p \leq 0.001$; ns / no markup: no
131 statistical difference.
132
133 **PKR is not blocked by DENV4 or ZIKV but shows delayed recognition dsRNA**
134 The late PKR activation during infection with both viruses is not explained by the need of
135 type I IFN signaling to boost PKR levels. Therefore, we tested whether PKR activity is blocked by
136 infection at earlier time points. To test this, the dsRNA analogue, poly (I:C), was used to stimulate PKR.
137 Poly (I:C) transfection was performed at 3 h p.i. and cells were analysed at 9 h p.i., that is, before virus-
138 promoted eIF2α phosphorylation (Figure 3A). The comparable levels of p–eIF2α between mock and
139 infected cells stimulated with poly (I:C) suggest that PKR is not blocked by DENV4 or ZIKV in the
140 early stages of infection (Figure 3A). The absence of p–eIF2α in $PKR^{-/-}$ cells demonstrates that eIF2α
141 phosphorylation induced by poly (I:C) is also dependent on this kinase.
142 If PKR is not blocked in the early stages of infection by DENV or ZIKV, the late ISR
143 activation could be due to the inability of RNA sensors such as PKR to access viral dsRNA, as
144 suggested previously [19–21]. To test this hypothesis, infected cells were incubated in a semisolid
145 medium so viral spread happens from cell to cell by juxtaposition allowing temporal inferences of
146 events based on cell location from the centre of the viral plaque. Immunofluorescence of DENV4
147 infected cells shows that cells at the edge of the viral plaque do not phosphorylate eIF2α despite the
148 presence of dsRNA (Figure 3B). This result indicates that ISR activation is delayed, occurring in
149 infected cells after the establishment of viral replication complexes.

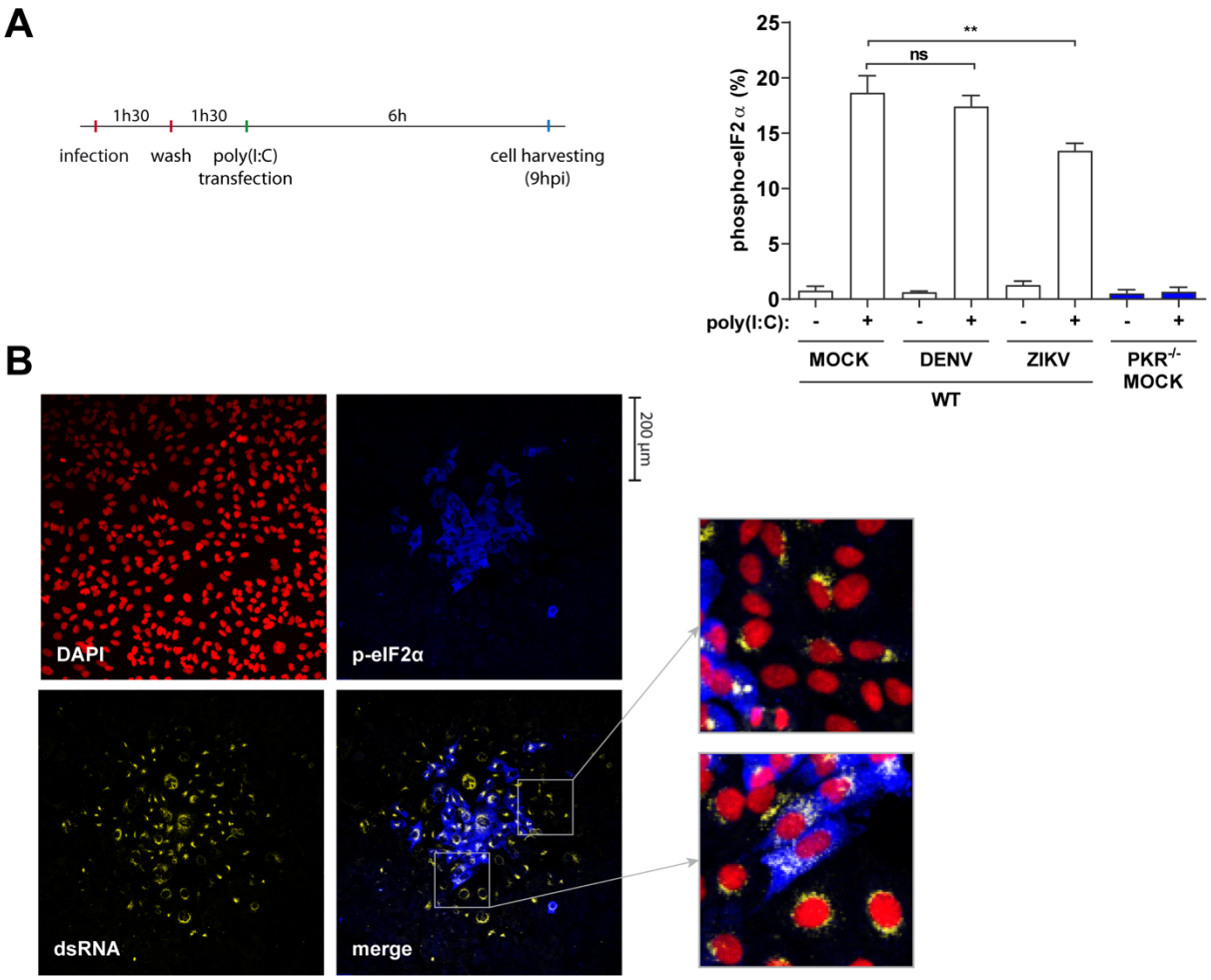

Figure 3 – PKR is not blocked by DENV4 or ZIKV but shows delayed recognition dsRNA. (A) Cells were infected with MOCK/DENV4/ZIKV and incubated for 1h30 before wash, then stimulated with poly (I:C) at 3 hpi with 10 µg/ml for 6 hours. Analysis for quantification of cell population expressing p–eIF2α after stimulation with poly (I:C) was performed by flow cytometry. Data obtained from three independent experiments. (B) Immunofluorescence of A549 WT cells infected with DENV4 for 48 h p.i. in semisolid medium. Cells fixed, permeabilized and co-stained with DAPI, anti-dsRNA and anti-p–eIF2α. Representative image of three independent experiments. In the column chart, bars represent the means ± SEM. Statistical analysis was performed by one-way ANOVA, followed by Tukey's test for multiple comparisons. *: $p \leq 0.05$; **: $p \leq 0.01$; ***: $p \leq 0.001$; ns / no markup: no statistical difference.

DENV4, but not ZIKV, induces translation arrest in infected cells

To investigate the consequences of eIF2α phosphorylation on cellular and viral protein translation, viral infections were performed in semi-solid medium and a puromycin labelling protocol was used to assess general translation activity [22]. By immunofluorescence analysis, it was possible to observe that p–eIF2α in WT lineage promotes cellular translation arrest during DENV4 infection,

167 evidenced by the absence of puromycin incorporation in the centre of viral plaques (Figure 4A). At the
168 edges of the plaque, however, anti-puromycin and anti-flavivirus simultaneous staining reinforces data
169 presented previously (Fig 3B) that translation arrest happens relatively late during DENV4 infection.
170 In $PKR^{-/-}$ cells, however, co-staining is present throughout the viral plaque, suggesting cell translation
171 downregulation during DENV4 infection is caused by ISR activation via PKR.

172 Surprisingly for ZIKV, there is a different profile, with more intense incorporation of
173 puromycin by infected WT cells than bystander cells (Figure 4B). Bystander cells are here defined as
174 cells that were in the same environment of infected cells (i.e., same well or organism) but viral protein
175 was not detected. Anti-puromycin signal is stronger in the perinuclear region which coincides with viral
176 replication sites (Figure 4C). The phenotype of increased translation activity in infected cells is lost in
177 $PKR^{-/-}$ cell lines, suggesting that PKR activation allows increased viral translation.

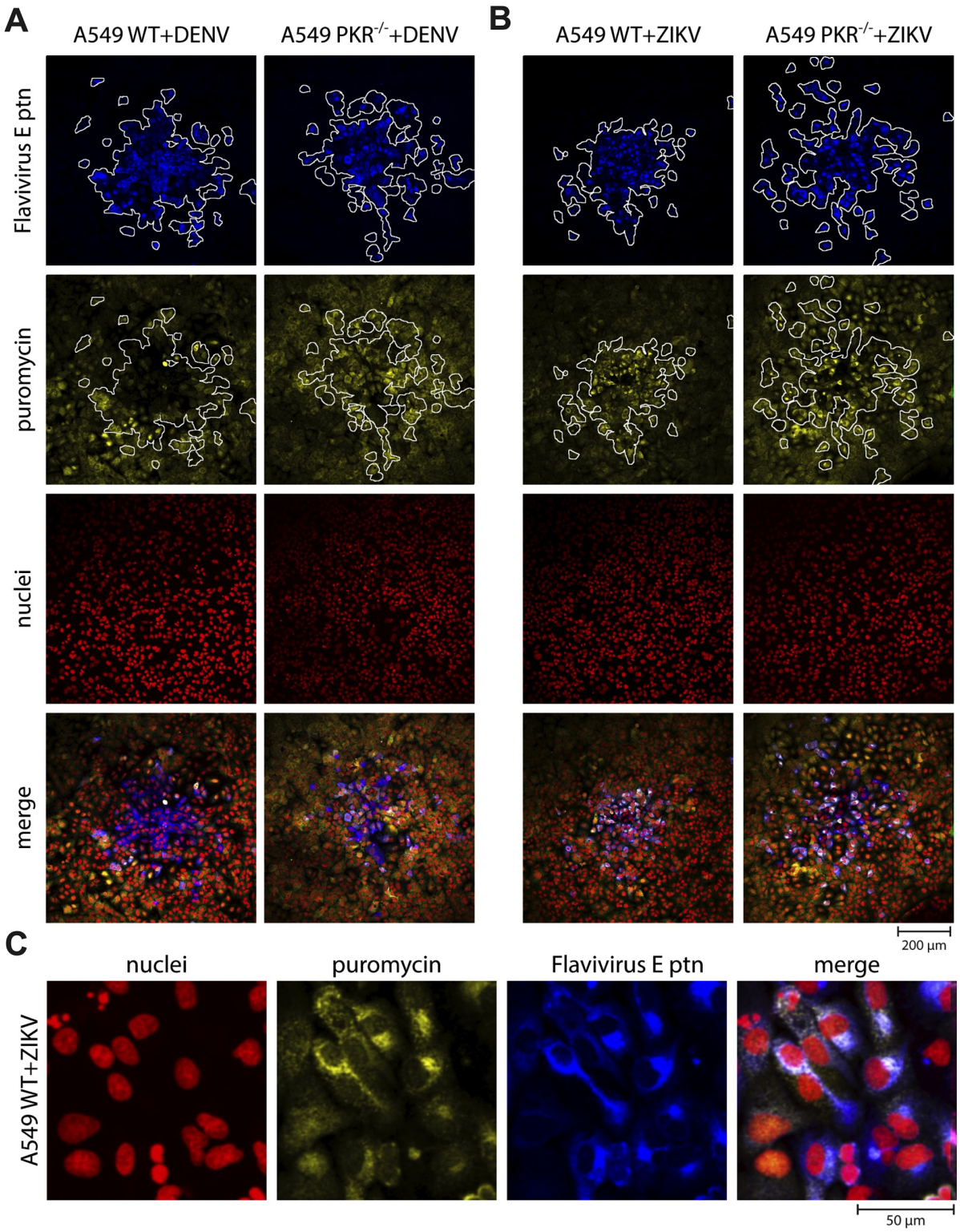

Figure 4 - DENV4, but not ZIKV, induces PKR-dependent translation arrest in infected cells. Immunofluorescence of A549 WT or PKR$^{-/-}$ cells infected with DENV4 (A) or ZIKV (B) for 48 h p.i. in semisolid medium. Cells labelled with puromycin before fixation and permeabilization. Co-staining with DAPI, anti-puromycin, anti-flavivirus envelope (E) and secondary antibodies. (C) Zoom on WT

183 cells infected with ZIKV for a better appreciation of the immunostaining pattern. Representative images
184 of three different experiments.
185
186 **PKR is required for expression of eIF2α-downstream genes and proteins during DENV4/ZIKV**
187 **infections**
188 Phosphorylation of eIF2α also leads to transcriptional up-regulation of genes from cellular
189 stress resolution pathways [23,24]. To evaluate the impact of PKR deficiency in events downstream of
190 eIF2α phosphorylation, the expression of *DDIT3* (CHOP) and *GADD34* was analysed. Gene
191 transcription was evaluated by qPCR (Figure 5A) and both *DDIT3* and *GADD34* were less expressed
192 in PKR$^{-/-}$ cells during DENV4/ZIKV infection than in WT cells. This downregulation is subtle, probably
193 due to control of these genes by other pathways such as IRF3/7 [25,26] and STAT3-NFkB or NF-YA
194 [27,28]. However, when GADD34 expression is analysed by immunoblot (Figure 5B) or flow
195 cytometry (Figure 5C) the downregulation of this protein follows p–eIF2α profile (Fig. 2A-B). These
196 results are in line with the literature since GADD34 mRNA translation requires p–eIF2α to suppress
197 uORF2 reading, which in turn inhibits the CDS translation [29,30], demonstrating the transcriptional
198 and post-transcriptional cellular control over eIF2α downstream signalling.
199 In summary, these results show that during infection by DENV4/ZIKV the activation of the
200 stress response is not restricted to phosphorylation of PKR and eIF2α; and reinforces that the activation
201 of this pathway is abolished in the PKR$^{-/-}$ cells.

202
203 **Figure 5 – PKR is required for expression of eIF2α-downstream genes and proteins during**
204 **DENV4/ZIKV infections.** A549 WT or PKR-/- cells infected with DENV4 (MOI 2) or ZIKV (MOI 3)
205 and harvested at 24 h p.i. for analysis. (A) Quantification by RT-qPCR of DDIT3 and GADD34 gene
206 expression. Relative expression calculated by 2-ΔΔCt methods using mock WT cells as reference. (B)
207 Immunoblot analysis of GADD34 protein expression. Representative image of two independent
208 experiments. (C) Flow cytometry analysis for quantification of cells expressing GADD34 within the
209 total population. In the column charts, bars represent the means ± SEM from three independent

experiments. Statistical analysis was performed by paired *t* test comparing the two cell lineages under the same conditions. *: p ≤0.05; **: p ≤0.01; ***: p ≤0.001; ns / no markup: no statistical difference.

Disruption of the PKR–eIF2α pathway impairs DENV4 and ZIKV replication

Considering the efficacy of p-eIF2α in blocking cellular translation and the dependency of PKR for this phosphorylation, we evaluated the impact of PKR deletion on virus replication. Surprisingly, replication of both viruses was impaired in PKR$^{-/-}$ cells, shown by lower virus titres (Figure 6A) and smaller plaque sizes and number of cells/plaque (Figure 6B-C). Viral genome replication, assessed by qPCR, does not show statistically significant difference, but a trend of lower replication in PKR$^{-/-}$ cells can be seen and may reflect impairment of other viral replication steps (Figure 6D).

The lower virus titres and diminished plaque sizes in PKR$^{-/-}$ cells are particularly counterintuitive since this cell line is defective in activating the whole antiviral pathway coordinated by PKR. This finding indicated the possibility that the PKR deletion has a negative impact on other antiviral pathways and/or these viruses could have co-opted the ISR to promote viral replication.

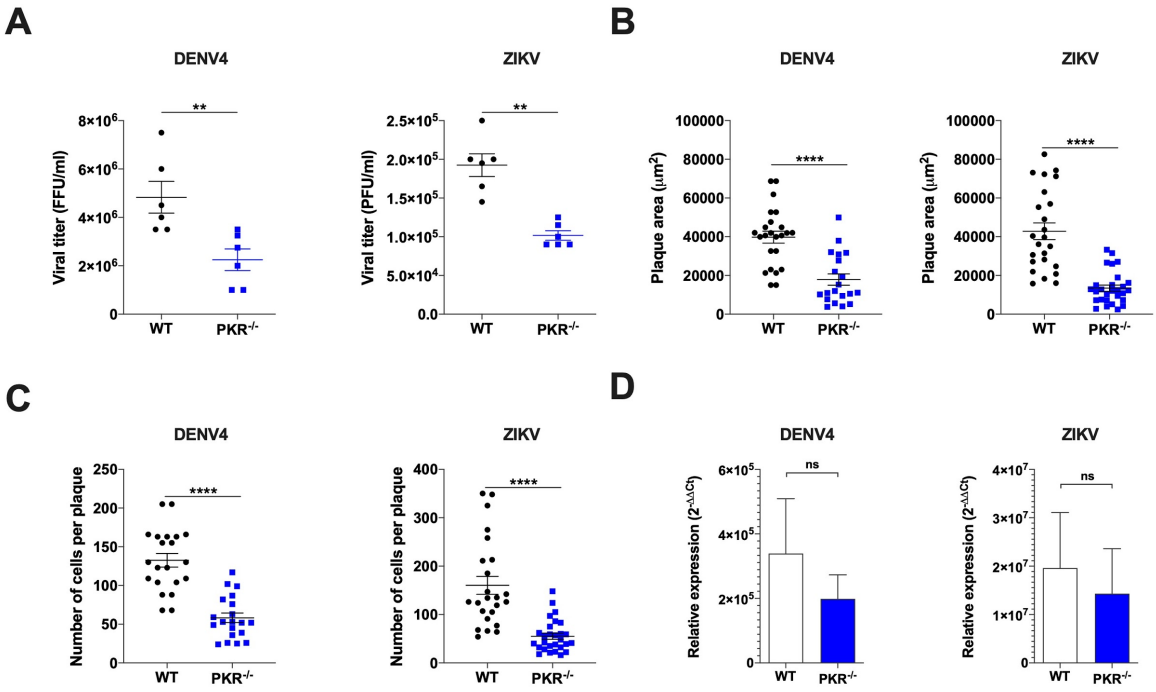

Figure 6 - Disruption of the PKR–eIF2α pathway impairs DENV4 and ZIKV replication. (A) Viral titration from A549 WT or PKR$^{-/-}$ cells infected with DENV4 (MOI 2) or ZIKV (MOI 3) and harvested at 24 h p.i. for analysis. Plaque size comparison of virus in A549 WT or PKR$^{-/-}$ cells infected with DENV4 and incubated for 8 days or infected with ZIKV and incubated for 5 days: measurements of (B) plaque areas and (C) number of cells per plaque from immunofluorescence. (D) Quantification by RT-

231 qPCR of DENV4 or ZIKV viral RNA from A549 WT or PKR$^{-/-}$ cells infected with DENV4 (MOI 2) or
232 ZIKV (MOI 3) and harvested at 24 h p.i. for analysis. Relative expression calculated by $2^{-\Delta\Delta Ct}$ method
233 using mock WT cells as a reference. PFU: plate forming units; FFU: focus forming units. In all charts,
234 bars represent the means ± SEM from three independent experiments. Statistical analysis was performed
235 by paired *t* test comparing the two cell lineages under the same conditions. *: $p \leq 0.05$; **: $p \leq 0.01$; ***:
236 $p \leq 0.001$; ns / no markup: no statistical difference.
237
238 **PKR deletion does not affect the innate immune response or cell viability**
239 The phenotype of reduced viral replication in PKR$^{-/-}$ lineage could be explained by changes
240 in the cellular innate immune response, as several studies report the role of PKR in sustaining NF-kB
241 and IFN signalling [31–36] and promoting IFNγ and TNFα expression [37,38]. To investigate the
242 possibility of alterations in innate immune pathways as a result of PKR deletion, gene and protein
243 expression of elements of this response was evaluated.
244 Genes activated by IRF3/7, IFN-I or NF-κB did not show any significant difference in
245 transcription between WT and PKR$^{-/-}$ lineages during virus infections (Figure 7A). Immunoblotting
246 corroborated this transcriptional analysis, as no differences were observed in STAT1 activation or IFIT1
247 and ISG15 expression levels between the two cell lines, thus demonstrating virus-induced IFN-I
248 signalling is not affected by PKR deletion (Figure 7B).
249 As PKR can also play a role in cell survival during viral infections [39], cell viability was
250 analysed at 24 h p.i. by cytometry. Also in this assay, no difference between WT and PKR$^{-/-}$ lineages
251 was observed during virus infections (Figure 7C).
252 Together, this set of results allow us to conclude that the PKR deletion does not significantly
253 affect the innate immune response or cell survival during DENV4 or ZIKV infection. Therefore,
254 alterations in these pathways do not explain the lower viral replication seen in the PKR$^{-/-}$ cells.

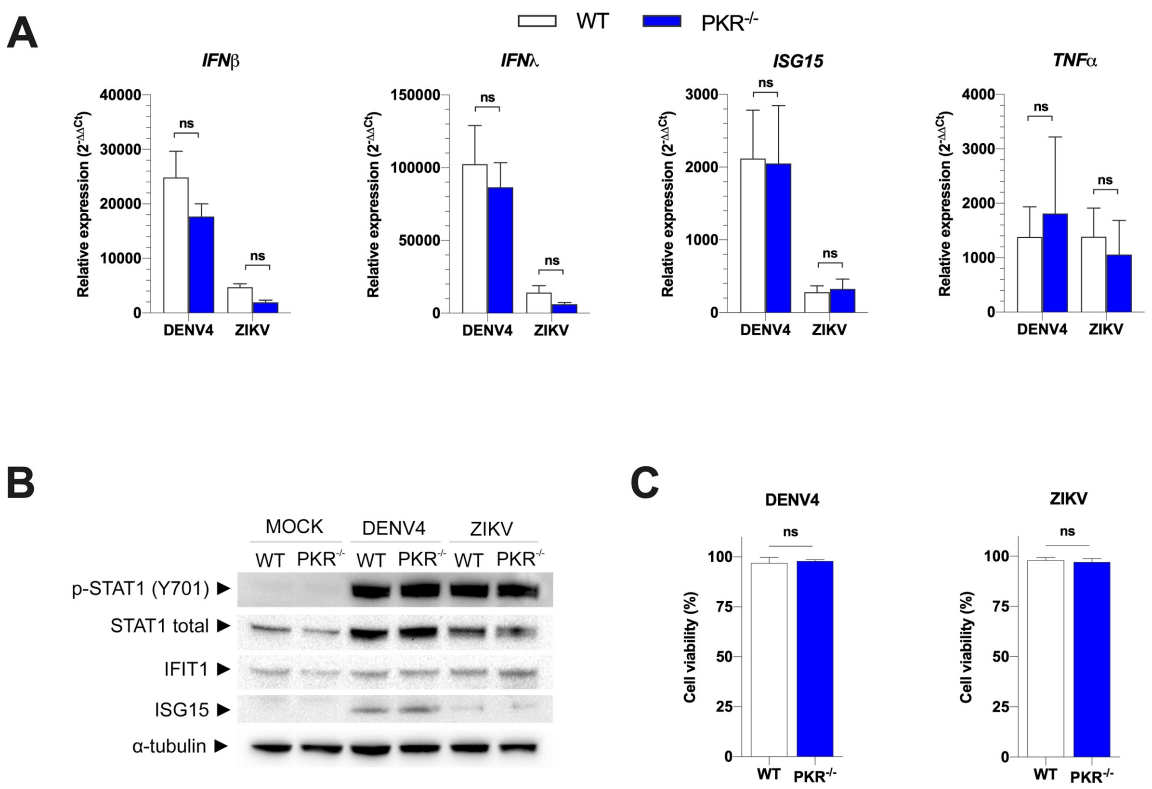

Figure 7 - PKR deletion does not affect the innate immune response or cell viability. A549 WT or PKR-/- cells infected with DENV4 (MOI 2) or ZIKV (MOI 3) and harvested at 24 h p.i. for analysis. (A) Quantification by RT-qPCR of IFNB, IFNL, ISG15 and TNFA1 gene expression. Relative expression calculated by 2-ΔΔCt methods using mock WT cells as a reference. (B) Immunoblot analysis of cell extracts resolved in denaturing SDS-PAGE. Representative image of two independent experiments. (C) Flow cytometry analysis for quantification of living cells by staining with Zombie-NIR viability dye. Mock WT cells set as 100% reference. In the column charts, bars represent the means ± SEM from three independent experiments. Statistical analysis was performed by paired *t* test comparing the two cell lineages under the same conditions. *: $p \leq 0.05$; **: $p \leq 0.01$; ***: $p \leq 0.001$; ns / no markup: no statistical difference.

ZIKV co-opts PKR–eIF2α pathway to increase viral translation through its 5´-UTR

ISR control over cell translation can promote the expression of certain mRNAs as a consequence of their 5´-UTR sequence and/or structure [30,40]. Therefore, we next sought to investigate whether viral 5´-UTR could subvert the ISR to promote replication. Hence, a translation activity assay was performed based on the ZIKV genome using a luciferase reporter readout. For this assay, a reporter plasmid was designed with the first 194 nucleotides of ZIKV, this includes the 5´-UTR followed by the first 87 nt from the viral polyprotein fused in frame with the firefly luciferase gene (Figure 8A). A control plasmid for expression of *Renilla* luciferase with the same backbone that the

275 firefly luciferase reporter was co-transfected for data normalization. Results are presented in Relative
276 Translation Activity (RTA), given in percentage, using values obtained with WT mock cells as
277 reference (100%).

278 Cells were infected with ZIKV for 12 hours before plasmid transfection, then analysed at 36
279 h p.i. to maximize the time of luciferase expression. The comparison between mock and infected
280 conditions for each cell line reveals that virus infection promotes a 2-fold increase in translation activity
281 by WT and IFNAR$^{-/-}$ cells (Figure 8B). In contrast, in PKR$^{-/-}$ and double knockout cells this effect is
282 suppressed as relative translation activity in these cells, under infected and uninfected conditions, is
283 similar or lower to WT uninfected cells. These results suggest that the ZIKV 5´-UTR is sufficient to
284 promote a relative advantage of mRNA translation in the presence of p–eIF2α.

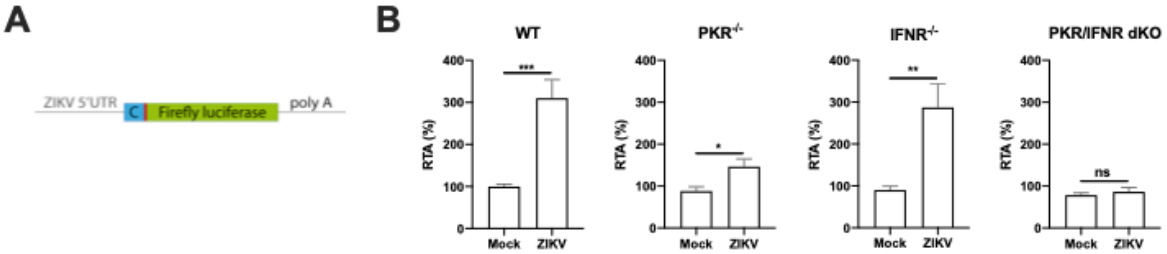

285

286 **Figure 8 - ZIKV 5´-UTR is sufficient to increase relative reporter translation in PKR–eIF2α**
287 **competent cells**. (A) Diagram of reporter construct used for the assay. (B) Relative translation of ZIKV
288 reporter in A549 (WT/PKR$^{-/-}$/IFNAR$^{-/-}$/DKO) cells infected with ZIKV (MOI 3), transfected at 12 h p.i.
289 and analysed at 36 h p.i. C: first 87 nt of viral capsid protein. In the column chart, the bars represent the
290 means ± SEM from three independent experiments. *: $p \leq 0.05$; **: $p \leq 0.01$; ***: $p \leq 0.001$; ns / no
291 markup: no statistical difference.

292

293 **DISCUSSION**

294 Given the *Flavivirus* genome structure, it is suggested that these viruses would use a cap-
295 dependent translation mechanism for viral polyprotein synthesis until the suppression of canonical
296 initiation machinery when a switch to cap-independent translation would take place [3,5]. Cell
297 conditions to promote the switch in translation mode and the required auxiliary factors (eIFs) for
298 alternative translation remain to be fully characterized.

299 In the present work, we investigated how ISR, known to promote translation arrest through
300 eIF2α phosphorylation, would play a role in this elusive non-canonical translation mechanism employed
301 by flaviviruses. Using A549 cells we verified that PKR promotes p-eIF2α during DENV4 and ZIKV
302 infections. In accordance, previous reports have also detected p-eIF2α in A549 cells during DENV
303 [6,41], ZIKV [42] and JEV [43] infections; as well as studies using other cell lines [44,45]. Further

304 characterization of p-eIF2α was performed by flow cytometry to allow quantification and co-staining
305 for other markers. Although DENV4 and ZIKV promote eIF2α phosphorylation within the same time
306 frame, these viruses displayed different profiles of anti–p–eIF2α and anti–flavivirus co-staining,
307 indicating distinct dynamics between viral replication and activation of stress response for each virus.
308 Therefore, cytometry is here proposed as a complementary method to investigate ISR activation, in
309 addition to traditionally used immunoblot and immunofluorescence, as it can provide more detailed
310 information.

311 It is worth noting that a few studies observe PERK/UPR activation during DENV and ZIKV
312 infections without excluding the participation of other ISR kinases especially regarding eIF2α
313 phosphorylation [46–50]. In the present model, PERK plays a minor role in ZIKV-induced p-eIF2α.
314 Here, PKR is clearly accountable for ISR activation during infection with both DENV4 and ZIKV. This
315 response was shown to be activated from PKR to p-eIF2α-downstream genes in WT lineage but
316 abolished in PKR$^{-/-}$ lineage. However, other flaviviruses such as JEV and WNV seem to phosphorylate
317 eIF2α at least partially dependent on PERK [46–50]. For JEV, this could be due to PKR blocking
318 promoted by viral NS2a [43].

319 An increased expression of p-eIF2α downstream genes was also found in Huh7 cells infected
320 with DENV [51]. In this study, single-cell RNA-seq analysis showed upregulation of *DDIT3* and
321 *GADD34* (aka *PPP1R15A*) mRNAs, as well as of other ATF4-downstream genes (*ASNS, CTH,*
322 *HERPUD1, SOD2, TRIB3*) [52–56] within the infected population (Supplementary Figure 3A-B). A
323 second study using the same approach in PBMC [57] revealed an upregulation of *GADD34* mRNA in
324 DENV-infected monocytes and T cells (Supplementary Figure 3C-D). The upregulation of these
325 mRNAs suggests ISR activation after DENV infection in these cell models. However, as shown here,
326 the expression of these genes is also regulated by post-transcriptional mechanisms dependent on the
327 presence of p-eIF2α.

328 In our model, a PKR-dependent translation arrest was confirmed in DENV-infected cells as
329 expected, but curiously not in ZIKV-infected cells. For the latter, increased puromycin incorporation in
330 perinuclear areas indicates a possible viral escaping mechanism from ISR translation control. This
331 difference might be related to the distinct dynamics between viral replication and activation of stress
332 response for each virus seen in the co-staining assay. Therefore, it calls for further investigation using
333 methods such as live-cell imaging, to track down the sequence of events during infection.

334 Roth et al, reported a general translation arrest after infection of Huh7 cells with several
335 *Flavivirus* species and strains despite the absence of p-eIF2α [7]. This conflicting result could be due
336 to the different cell lineage used. Although we do not exclude the possibility that other translation

337 suppression mechanisms, such as RIDD [58], RNase L [59] and 4E-BP dephosphorylation [60,61], can
338 also take place in our model in later times after infection.

339 Despite the differences in translational activity under activated ISR, both DENV4 and ZIKV
340 presented an approximated 50% less viral replication in PKR$^{-/-}$ cells. This decrease suggests that ISR
341 activation is not essential for viral replication but rather co-opted by both viruses to counter a major
342 cellular antiviral pathway for their own benefit. Indeed, after discarding the hypothesis of PKR deletion
343 disturbing common antiviral pathways in this model (e.g., type I IFN expression, NFκB activation and
344 apoptosis), translation activity assay has shown that ZIKV 5´-UTR promotes a relative advantage of
345 mRNA translation in the presence of p–eIF2α. This finding reveals that ZIKV not only escapes ISR
346 translation arrest, but also uses this response to increase viral replication. Moreover, it also indicates
347 that viral alternative translation does not require eIF2/TC for initiation. The independence of eIF2 for
348 translation initiation under stress conditions has been previously reported within *Flaviviridae* family,
349 since HCV (*Hepacivirus* genus) and *Pestivirus C*(formerly CSFV, *Pestivirus* genus) IRES present
350 similar functioning [62–64].

351 Here we demonstrate that DENV and ZIKV induce eIF2α phosphorylation in a PKR dependent
352 manner and that its absence is detrimental for optimal virus replication. Using ZIKV as a model we
353 showed that this effect maps to the 5'UTR of the viral genome. Altogether these results suggest that the
354 activation of the PKR/p-eIF2α axis may be necessary for the engagement of the non-canonical
355 translation employed by Flaviviruses.

356

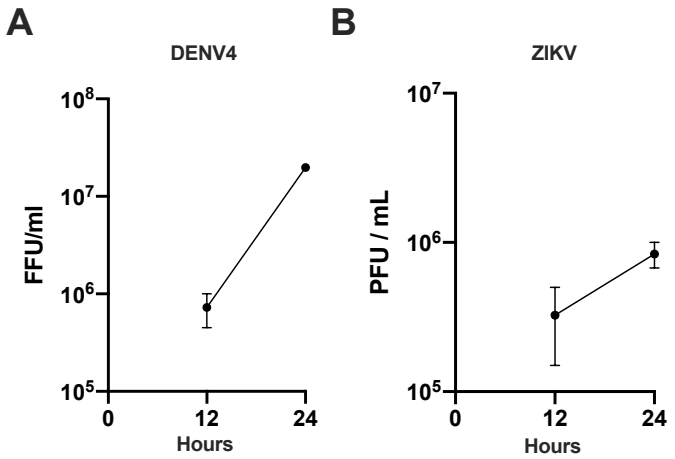

357

358

359 **Supplementary Figure 1** – Viral titration from A549 WT or PKR$^{-/-}$ cells infected with (A) DENV4
360 (MOI 2) or (B) ZIKV (MOI 3) and harvested at 12 and 24 h p.i. for analysis. PFU: plate forming units;
361 FFU: focus forming units. In all charts, points represent the means ± SEM from three independent
362 experiments.

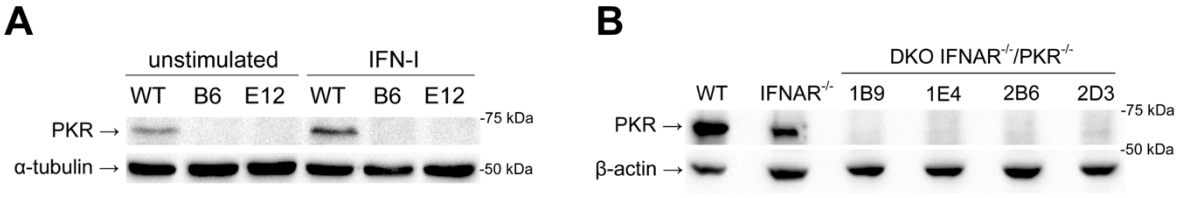

Supplementary Figure 2 – Characterization of knockout cell lines. (A) Clones of A549 PKR$^{-/-}$: Immunoblot of unstimulated and stimulated cells with 100 IU/ml of IFN-α2a for 12 hours demonstrating successful PKR deletion. (B) Clones of A549 IFNAR$^{-/-}$/PKR$^{-/-}$ after stimulation with 100 IU/ml of IFN-α2a for 12 hours demonstrating the deletion of PKR on the parental IFNAR$^{-/-}$ cells. DKO: double-knockout.

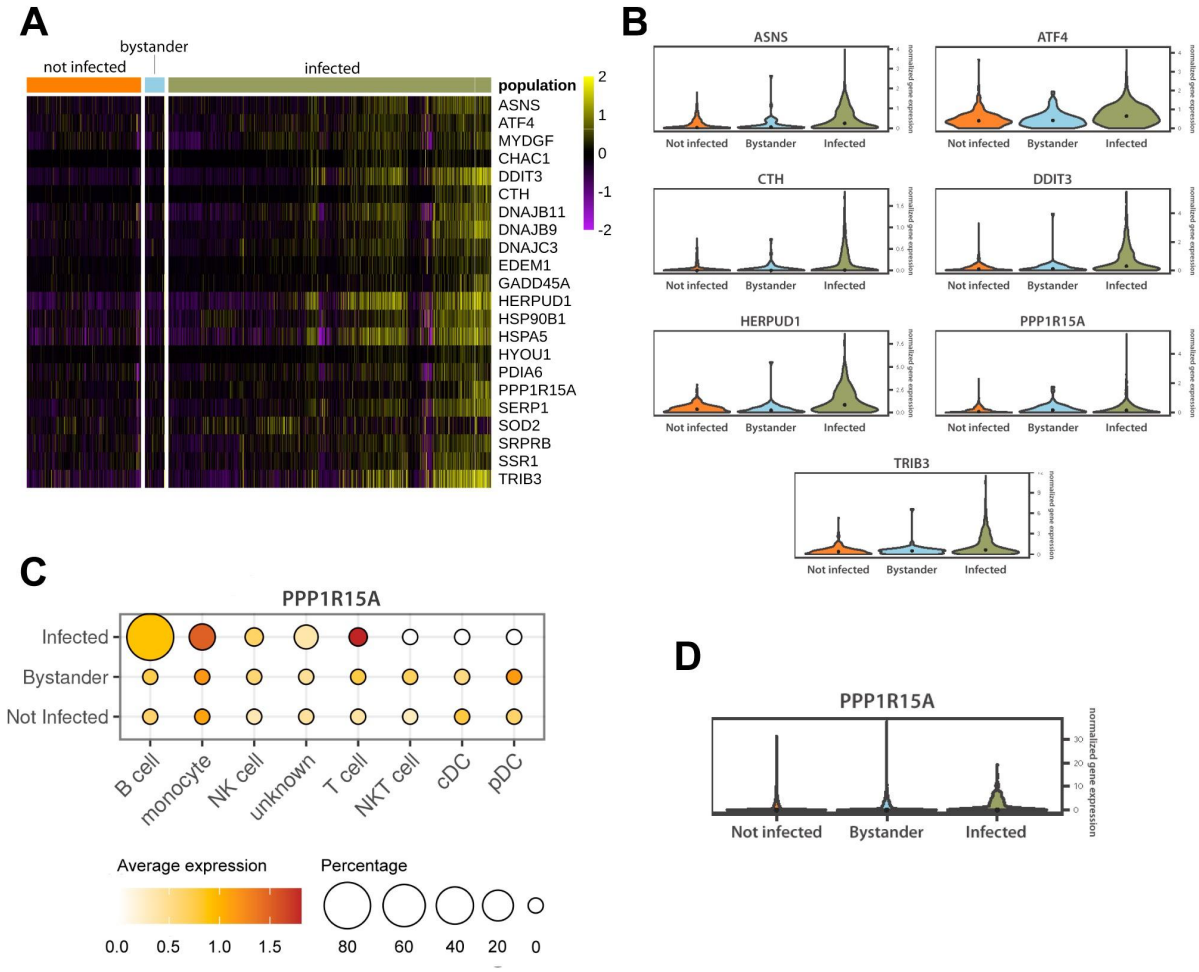

Supplementary figure 3 – p–eIF2α-downstream genes are upregulated in DENV-infected Huh7 cells and PBMCs. (A) Dataset from [51], of DENV-infected Huh7 cells, analysed by single-cell RNA-seq. Heatmap representing expression variability of stress-related genes in uninfected, bystander and infected cells; and (B) violin plot representing the expression of p-eIF2α- and ATF4-downstream genes

377 in uninfected, bystander and infected cell populations. (C) Dataset from [57], of PBMCs from patients
378 infected with DENV, analysed by single-cell RNA-seq. Dot plot representing the expression of
379 PPP1R15A/GADD34 in different cell population and infection conditions; and (D) violin plot
380 representing the expression of PPP1R15A/GADD34 the whole PBMC population under uninfected,
381 bystander and infected conditions.
382
383 **MATERIALS AND METHODS**
384 **Cells and viruses**. VERO-E6 (ATCC® CRL-1586™) A549 (ATCC® CCL-185™) and
385 derived cell lines were grown at 37° C/5% CO2 in DMEM-F12 medium supplemented with 1 U/ml
386 penicillin /streptomycin and 5% fetal bovine serum. C6/36 cells (ATCC® CRL-1660 were grown at
387 28° C in Leibovitz's L-15 medium supplemented with 1 U/ml penicillin /streptomycin and 5% fetal
388 bovine serum. IFNAR1 knockout cell line has been previously described [65,66]. PKR$^{-/-}$ and DKO
389 (IFNAR$^{-/-}$/PKR$^{-/-}$) were produced with a pair of sgRNA guides (PKR1-FWD:
390 CACCGATTATGAACAGTGTGCATCG; PKR1-REV: AAACCGATGCACACTGTTCATAATC;
391 PKR2-FWD:CACCGAAACAGTTCTTCGTTGCTTA; PKR2-REV:
392 AAACTAAGCAACGAAGAACTGTTTC) cloned into pSpCas9(BB)-2A-Puro (PX459) vector
393 (Addgene) according to developer's protocol [67]. Clonal populations of new cell lines were isolated
394 and tested to confirm gene deletion (Supplementary figure 2). Experiments were carried out with the
395 1B6 clone of PKR$^{-/-}$ cells and the 2B6 clone of DKO cells.
396 DENV-4 virus, TVP-360 strain (KUCZERA et al., 2016) and ZIKV, strain BR 2015/15261
397 (STROTTMANN et al., 2019) were kindly provided by Dr Claudia N. Duarte dos Santos (Fiocruz-PR,
398 Brazil). Viral stocks were produced in C6/36 cells and all viral titrations were performed in VERO cells
399 by plaque-forming units (PFU) or focus-forming units (FFU).
400 **Poly (I:C)Transfection**. Cell stimulation with poly (I:C) ("polyinosinic: polycytidylic acid")
401 was performed with Lipofectamine 3000 (Invitrogen) following manufacturer's instructions for A459
402 cells at the proportion of 1 ug of poly(I:C) in 1 ml of medium in a 12-well plate.
403 **Western-blots**. Samples were lysed on ice with RIPA buffer (150 mM NaCl; 50 mM Tris-
404 HCl pH8; 1% NP40; 0.1% SDS; 0.5% sodium deoxycholate) supplemented with cOmplete™ and
405 PhosSTOP inhibitors™ (Roche) according to manufacturer's recommendations. Protein extracts were
406 heat-denatured in the loading buffer and resolved in SDS-PAGE. Antibodies used for immunoblot
407 reactions were: PKR antibody (Santa Cruz Biotechnology, Inc, sc-707, dilution 1:100); phospho-PKR
408 (Thr451) polyclonal antibody, Invitrogen, 44-668G, dilution 1:100); phospho-eIF2α (Ser51) antibody
409 (Cell Signaling Technology, Inc., #9721, dilution 1:1000); GADD34 antibody (Proteintech, 10449-1-
410 AP, dilution 1:500); α-tubulin (DM1A) mAb (Cell Signaling Technology, Inc., #3873, dilution 1:1000);

411 STAT1 antibody (AbCam, ab3987, dilution 1:1000); phospho-STAT1(Y701) M135 (Abcam, ab29045,
412 dilution 1:1000); IFIT1 polyclonal antibody (Thermo/Pierce, PA3-848, dilution 1:1000); ISG15 mouse
413 mAb (R&D System, MAB4845, dilution 1:1000); anti-mouse IgG, HRP-linked Antibody (Cell
414 Signaling Technology, Inc., #7076, dilution 1:5000); anti-rabbit IgG, HRP-linked Antibody, Cell
415 Signaling Technology, Inc., #7074, dilution 1:5000). The imaging of blots was carried out on the
416 Chemidoc MP (Bio-Rad).

417 **Flow cytometry**. Cells were fixed in BD-Phosflow Lyse/Fix buffer. Primary and secondary
418 antibodies were diluted in permeabilization buffer (0.1% saponin; 1% fetal bovine serum, in PBS) for
419 staining. Between each step, samples were washed in blocking buffer (1% fetal bovine serum in PBS).
420 Antibodies and dyes used for flow cytometry were: phospho-eIF2α (Ser51) antibody (Cell Signaling
421 Technology, Inc., #3597, dilution 1:300); human monoclonal antibody DV 18.4 [68](dilution 1:100);
422 GADD34 antibody (Proteintech, 10449-1-AP, dilution 1:250 (IF/FACS); Zombie-NIR fixable viability
423 dye (BioLegend, 423105, dilution 1:750); Goat anti-Rabbit IgG (H+L) Alexa Fluor 647 conjugated
424 (Invitrogen, A-21245, dilution 1:500); Goat anti-Rabbit IgG (H+L) Alexa Fluor 488 conjugated
425 (Invitrogen, A-11008, dilution 1:500); Goat anti-Human IgG (H+L) Alexa Fluor 488 conjugated
426 (Invitrogen, A-11013, dilution 1:500). Data acquisition was performed with FACSVerse™ (BD) and
427 data analysis with FlowJo software (BD).

428 **Immunofluorescence**: Cells were grown and infected on 13 mm cover slips in 24-wells plates
429 and incubated in liquid or semisolid medium according to experiment design. Fixation in 3%
430 paraformaldehyde for 20 minutes and permeabilization with Triton X-100 0,5% in PBS for 5 minutes.
431 Primary and secondary antibodies were diluted in blocking buffer (2% bovine serum albumin in PBS)
432 for staining. Between each step, samples were washed in PBS. Antibodies and dyes used for
433 immunofluorescence were: DAPI (Invitrogen); anti-dsRNA MAb J2 (SCICONS, 10010500, dilution
434 1:200); human monoclonal antibody DV 18.4 [68](dilution 1:100); anti-puromycin 12D10 (Millipore,
435 MABE343, dilution 1:20,000); phospho-eIF2α (Ser51) antibody (Cell Signaling Technology, Inc.,
436 #3597, dilution 1:300); Goat anti-Rabbit IgG (H+L) Alexa Fluor 647 conjugated (Invitrogen, A-21245,
437 dilution 1:500); Goat anti-Rabbit IgG (H+L) Alexa Fluor 488 conjugated (Invitrogen, A-11008, dilution
438 1:500); Goat anti-Human IgG (H+L) Alexa Fluor 488 conjugated (Invitrogen, A-11013, dilution 1:500);
439 Donkey Anti-Mouse IgG H&L Alexa Fluor 647 conjugated (Abcam, ab150107, dilution 1:500). Image
440 acquisition was performed in the confocal microscope Leica DMI6000 B.

441 **RT-qPCR**:RNA was extracted and purified with HiYield TotalRNA mini kit (RBC Real
442 Biotech Corporation, YRB50) according to manufacturer's instructions. Reverse transcription reaction
443 was performed with MMLV "in house" kit from 1 µg of total RNA. Quantitative PCRs were performed
444 with GoTaq ® qPCR Master mix (Promega) with the following primer sets: h18S (F: 5'-

445 TAGAGGGACAAGTGGCGTTC-3', R: 5'-CGCTGAGCCAGTCAGTGT-3'); hIFNL1 (F: 5'-
446 TTCCAAGCCCACCACAACTG-3', R: 5'-GAGTGACTCTTCCAAGGCGT-3'); hIFNB1 (F: 5'-
447 AAACTCATGAGCAGTCTGCA-3', R: 5'-AGGAGATCTTCAGTTTCGGAGG-3'); hTNFA (F: 5'-
448 TCTTCTCGAACCCCGAGTGA-3', R: 5'-CCTCTGATGGCACCACCAG-3'); hISG15 (F: 5'-
449 TCCTGGTGAGGAATAACAAGGG-3', R: 5'-TCAGCCAGAACAGGTCGTC-3'); hDDIT3 (F: 5'-
450 GGAGCATCAGTCCCCCACTT-3', R: 5'-TGTGGGATTGAGGGTCACATC-3'); hGADD34 (F: 5'-
451 CTGGCTGGTGGAAGCAGTAA-3', R: 5'-TATGGGGGATTGCCAGAGGA-3'); DENV4 vRNA (F:
452 5'-TTGTCCTAATGATGCTGGTCG-3', R: 5'-TCCACCTGAGACTCCTTCCA-3'); ZIKV vRNA (F:
453 5'-CTGTGGCATGAACCCAATAG-3', R: 5'-ATCCCATAGAGCACCACTCC-3'). Data acquisition
454 with StepOne Plus real time PCR system (Applied Biosystems) and relative mRNA expression was
455 calculated by $2^{-\Delta\Delta CT}$ method.

456 **ZIKV Luciferase reporter vectors**: The pSGDLuc vector previously described [69], was
457 used as a template to design the *Renilla* luciferase and the ZIKV firefly luciferase reporters. The *Renilla*
458 luciferase was amplified using the following oligonucleotides 5´-
459 TCCGCCCAGTTCCGCCCATTCTCCGC-3´ and 5´-
460 GCGCTCTAGATTATCTCGAGGTGTAGAAATAC- 3´ and then cloned back into the pSGDLuc
461 previously digested with *AvrII* and *XbaI* This will create a plasmid only expressing the *Renilla*
462 luciferase gene under the T7 or SV40 promoter.
463 The first 194 nucleotides of the ZIKV genome were cloned first in the pSGD plasmid using the set of
464 primers 5´-GCGCCTCGAGATAAGTTGTTGATCTGTGTGAATCAGAC-3´ and 5´-
465 GCGCAGATCTGCCCCCAAAGGGGCTCACACGGGCTAC-3´ in order to introduce this fragment
466 in frame with the 2A-firefly luciferase gene. Using this intermediate plasmid as a template, the ZIKV-
467 2A-firefly luciferase gene was later amplified with oligonucleotides 5´-
468 TCCGCCCAGTTCCGCCCATTCTCCGC-3´and 5´-
469 GATTCACACAGATCAACAACTccctatagtgagtc to introduce the T7 promoter upstream of the ZIKV
470 coding region; and 5´-GCTTTACTGGGGCTACGATCTTTTGC-3´ and 5´-
471 gactcactatagggAGTTGTTGATCTGTGTGAATC-3´ to amplify the ZIKV region. This was cloned
472 back into the pSGD plasmid previously digested with *AvrII* and *BglII* . This will create a plasmid
473 expressing the ZIKV-2A-firefly luciferase fused gene under the T7 or SV40 promoter.

474 **Luciferase assays**: Cells were transfected using Lipofectamine 3000 (Invitrogen) with firefly
475 and *Renilla Luciferase* plasmids at the proportion of 98 ng and 2 ng respectively for every $2x10^4$ cells
476 in a 96-well plate. For cell lysis and luminescence reaction, Dual-Luciferase® Reporter Assay System
477 (Promega) was used following the manufacturer's instructions.
478

Single-cell RNA sequencing analysis: Processed, publicly available single-cell RNA-seq data are available through the GEO accession number GSE110496 and GSE116672. We downloaded processed single-cell data and metadata from the supplementary information from the respective publication [51,57].

Then, we used CellRouter [70] to perform quality control, normalization, analysis and visualize the expression of selected genes with log2 fold changes > 0.15.

AUTHOR CONTRIBUTIONS

Conceptualization, T.R.J. and D.S.M.; Methodology, T.R.J. and D.S.M.; Formal Analysis and Investigation, T.R.J.; *In silico* analysis, E.L.R., E.G.K., G.F.R.L.; Resources, D.S.M., B.F., N.I., Writing-Original Draft, T.R.J. and D.S.M., Writing-Review and editing, T.R.J., B.F., N.I. and D.S.M., Visualization, T.R.J. and D.S.M., Supervision, D.S.M., Project Administration and Funding Acquisition, D.S.M.

DECLARATION OF INTERESTS

The authors declare no competing interests.

ACKNOWLEDGEMENTS

This work was supported by Comissão de Aperfeiçoamento de Pessoal de Nível Superior (CAPES) Computational Biology programme (23038.010048/2013-27), Conselho Nacional de Desenvolvimento Científico e Tecnológico (CNPq) (1 311406/2017-3 and 407609/2018-0) and the Academy of Medical Sciences/U.K. (NAF004/1005) to D.S.M., Conselho Nacional de Desenvolvimento Científico e Tecnológico (CNPq) (41907/2017-7) to T.R.J., BBSRC grant BB/S001336/1 and Wellcome Trust grant 201946/Z/16/Z to B.J.F; and an Isaac Newton Trust Grant (18.40r), a Royal Society Research Grant (RGS\R1\191137) and an Isaac Newton Trust/Wellcome Trust ISSF/University of Cambridge Joint Research Grant to NI.

Multi-User Laboratory in Biological Studies (LAMEB) and LCME at UFSC.

REFERENCES

1. Chambers TJ, Hahn CS, Galler R, Rice CM (1990) Flavivirus genome organization, expression, and replication. *Annu Rev Microbiol* **44**: 649–688.
2. Gillespie LK, Hoenen A, Morgan G, Mackenzie JM (2010) The endoplasmic reticulum provides the membrane platform for biogenesis of the flavivirus replication complex. *J Virol* **84**: 10438–10447.
3. Edgil D, Polacek C, Harris E (2006) Dengue virus utilizes a novel strategy for translation initiation when cap-dependent translation is inhibited. *J Virol* **80**: 2976–2986.

513 4. Song Y, Mugavero J, Stauft CB, Wimmer E (2019) Dengue and Zika Virus 5' Untranslated
514 Regions Harbor Internal Ribosomal Entry Site Functions. *MBio* **10.**:
515 5. Fernández-García L, Angulo J, Ramos H, Barrera A, Pino K, Vera-Otarola J, López-Lastra M
516 (2020) The internal ribosome entry site of the Dengue virus mRNA is active when cap-
517 dependent translation initiation is inhibited. *J Virol*.
518 6. Hou J-N, Chen T-H, Chiang Y-H, Peng J-Y, Yang T-H, Cheng C-C, Sofiyatun E, Chiu C-H,
519 Chiang-Ni C, Chen W-J (2017) PERK Signal-Modulated Protein Translation Promotes the
520 Survivability of Dengue 2 Virus-Infected Mosquito Cells and Extends Viral Replication. *Viruses*
521 **9.**:
522 7. Roth H, Magg V, Uch F, Mutz P, Klein P, Haneke K, Lohmann V, Bartenschlager R, Fackler
523 OT, Locker N, et al. (2017) Flavivirus Infection Uncouples Translation Suppression from
524 Cellular Stress Responses. *MBio* **8.**:
525 8. Donnelly N, Gorman AM, Gupta S, Samali A (2013) The eIF2α kinases: their structures and
526 functions. *Cell Mol Life Sci* **70**: 3493–3511.
527 9. Pakos-Zebrucka K, Koryga I, Mnich K, Ljujic M, Samali A, Gorman AM (2016) The integrated
528 stress response. *EMBO Rep* **17**: 1374–1395.
529 10. Wek RC, Jiang H-Y, Anthony TG (2006) Coping with stress: eIF2 kinases and translational
530 control. *Biochem Soc Trans* **34**: 7–11.
531 11. Krishnamoorthy T, Pavitt GD, Zhang F (2001) Tight binding of the phosphorylated α subunit of
532 initiation factor 2 (eIF2α) to the regulatory subunits of guanine nucleotide exchange factor eIF2B
533 is required for …. *and cellular biology*.
534 12. Jackson RJ, Hellen CUT, Pestova TV (2010) The mechanism of eukaryotic translation initiation
535 and principles of its regulation. *Nat Rev Mol Cell Biol* **11**: 113–127.
536 13. Wang K, Zou C, Wang X, Huang C, Feng T, Pan W, Wu Q, Wang P, Dai J (2018) Interferon-
537 stimulated TRIM69 interrupts dengue virus replication by ubiquitinating viral nonstructural
538 protein 3. *PLoS Pathog* **14**: e1007287.
539 14. Whelan JN, Li Y, Silverman RH, Weiss SR (2019) Zika Virus Production Is Resistant to RNase
540 L Antiviral Activity. *J Virol* **93.**:
541 15. Gullberg RC, Steel JJ, Pujari V, Rovnak J, Crick DC, Perera R (2018) Stearoly-CoA desaturase 1
542 differentiates early and advanced dengue virus infections and determines virus particle
543 infectivity. *PLoS Pathog* **14**: e1007261.
544 16. Zhang J, Lan Y, Li MY, Lamers MM, Fusade-Boyer M, Klemm E, Thiele C, Ashour J, Sanyal S
545 (2018) Flaviviruses Exploit the Lipid Droplet Protein AUP1 to Trigger Lipophagy and Drive
546 Virus Production. *Cell Host Microbe* **23**: 819–831.e5.
547 17. Espada CE, da Rocha EL, dos Santos AA, Soares ZG, Malaquias G, Patrício DO, Kozlova EG,
548 dos Santos PF, Bordignon J, Sanford TJ, et al. (2019) ISG15/USP18/STAT2 is a molecular hub
549 regulating autocrine IFN I-mediated control of Dengue and Zika virus replication. *bioRxiv*.
550 18. Axten JM, Romeril SP, Shu A, Ralph J, Medina JR, Feng Y, Li WHH, Grant SW, Heerding DA,
551 Minthorn E, et al. (2013) Discovery of GSK2656157: An Optimized PERK Inhibitor Selected for
552 Preclinical Development. *ACS Med Chem Lett* **4**: 964–968.
553 19. Fredericksen BL, Gale M Jr (2006) West Nile virus evades activation of interferon regulatory
554 factor 3 through RIG-I-dependent and -independent pathways without antagonizing host defense
555 signaling. *J Virol* **80**: 2913–2923.
556 20. Espada-Murao LA, Morita K (2011) Delayed cytosolic exposure of Japanese encephalitis virus
557 double-stranded RNA impedes interferon activation and enhances viral dissemination in porcine
558 cells. *J Virol* **85**: 6736–6749.
559 21. Overby AK, Popov VL, Niedrig M, Weber F (2010) Tick-borne encephalitis virus delays
560 interferon induction and hides its double-stranded RNA in intracellular membrane vesicles. *J*
561 *Virol* **84**: 8470–8483.
562 22. Schmidt EK, Clavarino G, Ceppi M, Pierre P (2009) SUnSET, a nonradioactive method to
563 monitor protein synthesis. *Nat Methods* **6**: 275–277.
564 23. Harding HP, Novoa I, Zhang Y, Zeng H, Wek R, Schapira M, Ron D (2000) Regulated
565 translation initiation controls stress-induced gene expression in mammalian cells. *Mol Cell* **6**:
566 1099–1108.
567 24. Novoa I, Zeng H, Harding HP, Ron D (2001) Feedback Inhibition of the Unfolded Protein

568 Response by GADD34-Mediated Dephosphorylation of eIF2α. *J Cell Biol* **153**: 1011–1022.
569 25. Clavarino G, Cláudio N, Couderc T, Dalet A, Judith D, Camosseto V, Schmidt EK, Wenger T,
570 Lecuit M, Gatti E, et al. (2012) Induction of GADD34 is necessary for dsRNA-dependent
571 interferon-β production and participates in the control of Chikungunya virus infection. *PLoS*
572 *Pathog* **8**: e1002708.
573 26. Dalet A, Argüello RJ, Combes A, Spinelli L, Jaeger S, Fallet M, Vu Manh T-P, Mendes A,
574 Perego J, Reverendo M, et al. (2017) Protein synthesis inhibition and GADD34 control IFN-β
575 heterogeneous expression in response to dsRNA. *EMBO J* **36**: 761–782.
576 27. Huang Y, Chuang AY, Romano R-A, Liégeois NJ, Sinha S, Trink B, Ratovitski E, Sidransky D
577 (2010) Phospho-DeltaNp63alpha/NF-Y protein complex transcriptionally regulates DDIT3
578 expression in squamous cell carcinoma cells upon cisplatin exposure. *Cell Cycle* **9**: 328–338.
579 28. Canino C, Luo Y, Marcato P, Blandino G, Pass HI, Cioce M (2015) A STAT3-
580 NFkB/DDIT3/CEBPβ axis modulates ALDH1A3 expression in chemoresistant cell
581 subpopulations. *Oncotarget* **6**: 12637–12653.
582 29. Lee Y-Y, Cevallos RC, Jan E (2009) An upstream open reading frame regulates translation of
583 GADD34 during cellular stresses that induce eIF2alpha phosphorylation. *J Biol Chem* **284**:
584 6661–6673.
585 30. Young SK, Willy JA, Wu C, Sachs MS, Wek RC (2015) Ribosome Reinitiation Directs Gene-
586 specific Translation and Regulates the Integrated Stress Response. *J Biol Chem* **290**: 28257–
587 28271.
588 31. Gilfoy FD, Mason PW (2007) West Nile virus-induced interferon production is mediated by the
589 double-stranded RNA-dependent protein kinase PKR. *J Virol* **81**: 11148–11158.
590 32. Zamanian-Daryoush M, Mogensen TH, DiDonato JA, Williams BR (2000) NF-kappaB
591 activation by double-stranded-RNA-activated protein kinase (PKR) is mediated through NF-
592 kappaB-inducing kinase and IkappaB kinase. *Mol Cell Biol* **20**: 1278–1290.
593 33. Czerkies M, Korwek Z, Prus W, Kochańczyk M, Jaruszewicz-Błońska J, Tudelska K, Błoński S,
594 Kimmel M, Brasier AR, Lipniacki T (2018) Cell fate in antiviral response arises in the crosstalk
595 of IRF, NF-κB and JAK/STAT pathways. *Nat Commun* **9**: 493.
596 34. Deb A, Haque SJ, Mogensen T, Silverman RH, Williams BR (2001) RNA-dependent protein
597 kinase PKR is required for activation of NF-kappa B by IFN-gamma in a STAT1-independent
598 pathway. *J Immunol* **166**: 6170–6180.
599 35. Kårehed K, Dimberg A, Dahl S, Nilsson K, Oberg F (2007) IFN-gamma-induced upregulation of
600 Fcgamma-receptor-I during activation of monocytic cells requires the PKR and NFkappaB
601 pathways. *Mol Immunol* **44**: 615–624.
602 36. Li Y, Xie J, Wu S, Xia J, Zhang P, Liu C, Zhang P, Huang X (2013) Protein kinase regulated by
603 dsRNA downregulates the interferon production in dengue virus- and dsRNA-stimulated human
604 lung epithelial cells. *PLoS One* **8**: e55108.
605 37. Kaempfer R, Ilan L, Cohen-Chalamish S, Turgeman O, Namer LS, Osman F (2019) Control of
606 mRNA Splicing by Intragenic RNA Activators of Stress Signaling: Potential Implications for
607 Human Disease. *Front Genet* **10**: 464.
608 38. Ben-Asouli Y, Banai Y, Pel-Or Y, Shir A, Kaempfer R (2002) Human interferon-gamma mRNA
609 autoregulates its translation through a pseudoknot that activates the interferon-inducible protein
610 kinase PKR. *Cell* **108**: 221–232.
611 39. Donzé O, Deng J, Curran J, Sladek R, Picard D, Sonenberg N (2004) The protein kinase PKR: a
612 molecular clock that sequentially activates survival and death programs. *EMBO J* **23**: 564–571.
613 40. Young SK, Wek RC (2016) Upstream Open Reading Frames Differentially Regulate Gene-
614 specific Translation in the Integrated Stress Response. *J Biol Chem* **291**: 16927–16935.
615 41. Umareddy I, Pluquet O, Wang QY, Vasudevan SG, Chevet E, Gu F (2007) Dengue virus
616 serotype infection specifies the activation of the unfolded protein response. *Virol J* **4**: 91.
617 42. Hou S, Kumar A, Xu Z, Airo AM, Stryapunina I, Wong CP, Branton W, Tchesnokov E, Götte
618 M, Power C, et al. (2017) Zika Virus Hijacks Stress Granule Proteins and Modulates the Host
619 Stress Response. *J Virol* **91.**:
620 43. Tu Y-C, Yu C-Y, Liang J-J, Lin E, Liao C-L, Lin Y-L (2012) Blocking double-stranded RNA-
621 activated protein kinase PKR by Japanese encephalitis virus nonstructural protein 2A. *J Virol* **86**:
622 10347–10358.

44. Peña J, Harris E (2011) Dengue virus modulates the unfolded protein response in a time-dependent manner. *J Biol Chem* **286**: 14226–14236.
45. Tan Z, Zhang W, Sun J, Fu Z, Ke X, Zheng C, Zhang Y, Li P, Liu Y, Hu Q, et al. (2018) ZIKV infection activates the IRE1-XBP1 and ATF6 pathways of unfolded protein response in neural cells. *J Neuroinflammation* **15**: 275.
46. Gladwyn-Ng I, Cordón-Barris L, Alfano C, Creppe C, Couderc T, Morelli G, Thelen N, America M, Bessières B, Encha-Razavi F, et al. (2018) Stress-induced unfolded protein response contributes to Zika virus-associated microcephaly. *Nat Neurosci* **21**: 63–71.
47. Datan E, Roy SG, Germain G, Zali N, McLean JE, Golshan G, Harbajan S, Lockshin RA, Zakeri Z (2016) Dengue-induced autophagy, virus replication and protection from cell death require ER stress (PERK) pathway activation. *Cell Death Dis* **7**: e2127.
48. Wang Q, Xin X, Wang T, Wan J, Ou Y, Yang Z, Yu Q, Zhu L, Guo Y, Wu Y, et al. (2019) Japanese Encephalitis Virus Induces Apoptosis and Encephalitis by Activating the PERK Pathway. *J Virol* **93.**:
49. Sharma M, Bhattacharyya S, Sharma KB, Chauhan S, Asthana S, Abdin MZ, Vrati S, Kalia M (2017) Japanese encephalitis virus activates autophagy through XBP1 and ATF6 ER stress sensors in neuronal cells. *J Gen Virol* **98**: 1027–1039.
50. Ambrose RL, Mackenzie JM (2011) West Nile virus differentially modulates the unfolded protein response to facilitate replication and immune evasion. *J Virol* **85**: 2723–2732.
51. Zanini F, Pu S-Y, Bekerman E, Einav S, Quake SR (2018) Single-cell transcriptional dynamics of flavivirus infection. *Elife* **7.**:
52. Gjymishka A, Su N, Kilberg MS (2009) Transcriptional induction of the human asparagine synthetase gene during the unfolded protein response does not require the ATF6 and IRE1/XBP1 arms of the pathway. *Biochem J* **417**: 695–703.
53. Dickhout JG, Carlisle RE, Jerome DE, Mohammed-Ali Z, Jiang H, Yang G, Mani S, Garg SK, Banerjee R, Kaufman RJ, et al. (2012) Integrated stress response modulates cellular redox state via induction of cystathionine γ-lyase: cross-talk between integrated stress response and thiol metabolism. *J Biol Chem* **287**: 7603–7614.
54. Ma Y, Hendershot LM (2004) Herp is dually regulated by both the endoplasmic reticulum stress-specific branch of the unfolded protein response and a branch that is shared with other cellular stress pathways. *J Biol Chem* **279**: 13792–13799.
55. Fusakio ME, Willy JA, Wang Y, Mirek ET, Al Baghdadi RJT, Adams CM, Anthony TG, Wek RC (2016) Transcription factor ATF4 directs basal and stress-induced gene expression in the unfolded protein response and cholesterol metabolism in the liver. *Mol Biol Cell* **27**: 1536–1551.
56. Ohoka N, Yoshii S, Hattori T, Onozaki K, Hayashi H (2005) TRB3, a novel ER stress-inducible gene, is induced via ATF4-CHOP pathway and is involved in cell death. *EMBO J* **24**: 1243–1255.
57. Zanini F, Robinson ML, Croote D, Sahoo MK, Sanz AM, Ortiz-Lasso E, Albornoz LL, Rosso F, Montoya JG, Goo L, et al. (2018) Virus-inclusive single-cell RNA sequencing reveals the molecular signature of progression to severe dengue. *Proc Natl Acad Sci U S A* **115**: E12363–E12369.
58. Hollien J, Weissman JS (2006) Decay of endoplasmic reticulum-localized mRNAs during the unfolded protein response. *Science* **313**: 104–107.
59. Donovan J, Rath S, Kolet-Mandrikov D, Korennykh A (2017) Rapid RNase L-driven arrest of protein synthesis in the dsRNA response without degradation of translation machinery. *RNA* **23**: 1660–1671.
60. Pause A, Belsham GJ, Gingras AC, Donzé O, Lin TA, Lawrence JC Jr, Sonenberg N (1994) Insulin-dependent stimulation of protein synthesis by phosphorylation of a regulator of 5'-cap function. *Nature* **371**: 762–767.
61. Poulin F, Gingras AC, Olsen H, Chevalier S, Sonenberg N (1998) 4E-BP3, a new member of the eukaryotic initiation factor 4E-binding protein family. *J Biol Chem* **273**: 14002–14007.
62. Pestova TV, de Breyne S, Pisarev AV, Abaeva IS, Hellen CUT (2008) eIF2-dependent and eIF2-independent modes of initiation on the CSFV IRES: a common role of domain II. *EMBO J* **27**: 1060–1072.
63. Robert F, Kapp LD, Khan SN, Acker MG, Kolitz S, Kazemi S, Kaufman RJ, Merrick WC,

678 Koromilas AE, Lorsch JR, et al. (2006) Initiation of protein synthesis by hepatitis C virus is
679 refractory to reduced eIF2.GTP.Met-tRNA(i)(Met) ternary complex availability. *Mol Biol Cell*
680 **17**: 4632–4644.
681 64. Rivas-Estilla AM, Svitkin Y, Lopez Lastra M, Hatzoglou M, Sherker A, Koromilas AE (2002)
682 PKR-dependent mechanisms of gene expression from a subgenomic hepatitis C virus clone. *J*
683 *Virol* **76**: 10637–10653.
684 65. Antunes KH, Fachi JL, de Paula R, da Silva EF, Pral LP, Dos Santos AÁ, Dias GBM, Vargas JE,
685 Puga R, Mayer FQ, et al. (2019) Microbiota-derived acetate protects against respiratory syncytial
686 virus infection through a GPR43-type 1 interferon response. *Nat Commun* **10**: 3273.
687 66. Guimarães ES, Gomes MTR, Campos PC, Mansur DS, Dos Santos AA, Harms J, Splitter G,
688 Smith JA, Barber GN, Oliveira SC (2019) Cyclic Dinucleotides Trigger STING-Dependent
689 Unfolded Protein Response That Favors Bacterial Replication. *J Immunol* **202**: 2671–2681.
690 67. Ran FA, Hsu PD, Wright J, Agarwala V, Scott DA, Zhang F (2013) Genome engineering using
691 the CRISPR-Cas9 system. *Nat Protoc* **8**: 2281–2308.
692 68. Beltramello M, Williams KL, Simmons CP, Macagno A, Simonelli L, Quyen NTH, Sukupolvi-
693 Petty S, Navarro-Sanchez E, Young PR, de Silva AM, et al. (2010) The human immune response
694 to Dengue virus is dominated by highly cross-reactive antibodies endowed with neutralizing and
695 enhancing activity. *Cell Host Microbe* **8**: 271–283.
696 69. Loughran G, Howard MT, Firth AE, Atkins JF (2017) Avoidance of reporter assay distortions
697 from fused dual reporters. *RNA* **23**: 1285–1289.
698 70. Lummertz da Rocha E, Rowe RG, Lundin V, Malleshaiah M, Jha DK, Rambo CR, Li H, North
699 TE, Collins JJ, Daley GQ (2018) Reconstruction of complex single-cell trajectories using
700 CellRouter. *Nat Commun* **9**: 892.

701